Characterization of binding and structural properties of rat liver fatty-acid-binding protein using tryptophan mutants

Alfred E. A. THUMSER and David C. WILTON*
Department of Biochemistry, University of Southampton, Bassett Crescent East, Southampton SO9 3TU, U.K.

Rat liver fatty-acid-binding protein (FABP) does not contain tryptophan. Three mutant proteins have been produced in which a single tryptophan residue has been inserted by site-directed mutagenesis at positions 3 (F3W), 18 (F18W) and 69 (C69W). These tryptophans have been strategically located in order to provide fluorescent reporter groups to study the binding and structural characteristics of rat liver FABP. Two fluorescent fatty acid analogues, DAUDA {11-[(5-dimethylaminonaphthalene-1-sulphonyl)amino]undecanoic acid} and 3-[*p*-(6-phenyl)-hexa-1,3,5-trienyl]phenylpropionic acid, showed no significant difference in binding affinities for the different mutant proteins, although maximum fluorescence values were decreased for F3W and increased for C69W. These findings were confirmed by studies of DAUDA displacement by oleate. Protein-denaturation studies in the presence of urea indicated subtle differences for the three mutants which could be explained by multiple unfolding pathways. Fatty acid binding increased tryptophan fluorescence emission in the case of the F18W protein, but had no effect on the F3W and C69W proteins. Fluorescence quenching studies with 2-bromopalmitate showed that a fatty acid carboxylate is close to the tryptophan in the F18W protein. Energy-transfer studies showed that the fluorescent moiety of DAUDA is equidistant from the three mutated amino acids and is bound within the β-clam solvent cavity of liver FABP. This interpretation of the fluorescence quenching and energy-transfer data supports the difference in ligand orientation between intestinal and liver FABP observed in previous studies.

INTRODUCTION

The fatty acid-binding proteins (FABPs) are widely distributed cytosolic hydrophobic ligand-binding proteins of low molecular mass found at relatively high concentrations in liver, heart and intestine [1–3]. The main endogenous ligands are fatty acids of C_{16}–C_{22} chain length, although other lipids and carcinogens bind with lower affinity [2,3]. The following functions for FABP have been suggested: (a) fatty acid uptake and transport, (b) protection of membranes against the detrimental effects of high levels of fatty acids and their metabolites and (c) regulation of various fatty acid metabolic pathways. However, these functions are based mainly on indirect evidence, and the exact physiological role of these proteins remains unknown [2–4].

Rat liver FABP differs from the heart and intestinal isoforms in the general characterization of ligand binding and specificity. The liver isoform is commonly accepted to bind a molar ratio of two fatty acid molecules, whereas the intestinal form only binds one fatty acid [5–8]. In the latter protein the fatty acid carboxylate is also involved in electrostatic interactions with amino acid side chains [1,9], while n.m.r. studies indicate that such interactions do not occur with liver FABP, and in this case the fatty acid carboxylates are solvent-accessible and located near the protein/solvent interface [6,7]. Furthermore, liver FABP is able to bind a wide range of ligands [3], including, among others, lipid metabolites such as acyl-CoA [10,11] and lysophosphatidylcholine (lysoPC) [12]. Jakoby et al. [13] have suggested that cytosolic lipid-binding proteins can be separated into two subgroups based on sequence alignments and the presence or absence of the arginine found at position 106 in intestinal FABP. Thus intestinal and heart or muscle FABP, the last two being identical [14], contain this vital arginine, whereas liver FABP contains a threonine residue at the same position [13]. The subgroup containing liver FABP can bind a wider variety of ligands, whereas the alternative group is more ligand specific [13].

The crystallographic structures of various FABPs show a basic tertiary structure consisting of ten anti-parallel β-sheets, organized into two approximately orthogonal β-sheets forming a β-clam configuration, and two α-helices forming part of a proposed portal region [1,9,15,16]. The fatty acid carboxylate forms electrostatic interactions with Arg-106 in intestinal FABP and the acyl chain extends towards the portal region, surrounded by the side chains of hydrophobic amino acids [1]. No structure for rat liver FABP has been published.

Using site-directed mutagenesis techniques we have replaced three amino acids in rat liver FABP, i.e. Phe-3, Phe-18 and Cys-69, with tryptophans to facilitate structural and binding studies using fluorescent techniques. Cys-69 was chosen for mutation as it has been shown that ligand binding is not affected by modification of this unique cysteine with dithionitrobenzene (DTNB) or *N*-iodoacetyl-*N'*-(5-sulpho-1-naphthyl)ethylenediamine ('IAEDANS') [17,18]. Ligand binding and denaturation studies displayed distinct effects for the three mutants, while energy-transfer studies indicated that the fluorescent moiety of the fatty acid analogue, 11-[(5-dimethylaminonaphthalene-1-sulphonyl)amino]undecanoic acid (DAUDA), was bound in the β-clam binding pocket.

MATERIALS AND METHODS

Materials

9(10)-Bromostearic acid, oleoyl-CoA, oleoyl-lysoPC and fatty acids (Sigma Chemical Co., St. Louis, MO, U.S.A.); DAUDA,

Abbreviations used: DAUDA, 11-[(5-dimethylaminonaphthalene-1-sulphonyl)amino]undecanoic acid; DPH-PA, 3-[*p*-(6-phenyl)hexa-1,3,5-trienyl]-phenylpropionic acid; DTNB, dithionitrobenzene; FABP, fatty-acid-binding protein; lysoPC, lysophosphatidylcholine.

* To whom correspondence should be sent.

3-[*p*-(6-phenyl)hexa-1,3,5-trienyl]phenylpropionic acid (DPH-PA), *cis*-parinaric acid (Molecular Probes, Eugene, OR, U.S.A.); isopropyl β-D-thiogalactoside (Northumbria Biologicals, Cramlington, Northd., U.K.); 2-bromopalmitate (2-bromohexadecanoic acid) (Aldrich Chemie, Steinheim, Germany).

All other chemicals were of analytical grade quality.

Mutagenesis and cloning

The FABP gene has been cloned into a modified pET-11 vector [11] and three mutants (Phe-3 to Trp-3: F3W; Phe-18 to Trp-18: F18W; Cys-69 to Trp-69: C69W) produced by site-directed mutagenesis using a M13 phage vector and standard cloning techniques [19–21]. The relevant mutations were verified by DNA sequencing [22] and the plasmids were transformed into BL21 DE3 cells [21].

Protein purification

Overnight cultures grown in DYT medium (16 g of tryptone, 10 g of yeast extract, 5 g of NaCl per litre of medium, pH 7.2) containing ampicillin (50 μg/ml) [23] were diluted into the same medium and grown for 2.5 h before induction with 0.5 mM isopropyl β-D-thiogalactoside for 4–6 h. The cells were collected and the FABP purified from sonicated cells by $(NH_4)_2SO_4$ fractionation and chromatography on naphthylaminodecyl–agarose and Sephadex G-75, as previously described [17,24]. The proteins were de-lipidated on Lipidex 1000 [25] and concentrated using an Amicon YM3 membrane.

Protein concentrations were determined by a dye-binding assay [26]. The proteins were essentially pure on SDS/PAGE [27].

General methods

Concentrations of fluorescent fatty acid probes were determined by their absorption coefficients: ε_{335} (DAUDA) = 4400 $M^{-1}\cdot cm^{-1}$ in methanol [28], ε_{360} (DPH-PA) = 60000 $M^{-1}\cdot cm^{-1}$ in egg phosphatidylcholine vesicles [29], ε_{304} (*cis*-parinaric acid) = 79000 $M^{-1}\cdot cm^{-1}$ in methanol [30]. The absorbance spectrum of DPH-PA is not dependent on solvent polarity [31], and DPH-PA concentrations were determined in methanol.

All absorbance and fluorescence determinations were corrected for buffer and DAUDA (as relevant). Fluorescence emission spectra were corrected using tryptophan as a standard, with tryptophan concentrations determined by using the absorption coefficient: ε_{280} = 5600 $M^{-1}\cdot cm^{-1}$ [32]. All fluorescence measurements were determined in 50 mM Hepes buffer, pH 7.5, at 25 °C. Methanol concentrations, where appropriate, were kept constant at 1% (v/v) for determination of binding kinetics.

All relevant data are shown as means ± S.D. Statistical significance was determined by Student's *t* test.

Inner-filter effects

Corrections for inner-filter effects (in the case of DPH-PA and oleoyl-CoA) were made by using eqn. (1) or by using a standard curve [33]. Both methods gave essentially the same results.

$$F_{correct} \approx F_{observed} \exp[(A_{excitation} + A_{emission})/2] \quad (1)$$

where F is the fluorescence emission and A the absorbance of the solution at the excitation and emission wavelengths respectively.

All other fluorophores were used at concentrations for which absorbances were below 0.05 [33].

Fluorescence quenching

Fluorescence quenching data was fitted to the classical Stern–Volmer equation [34]:

$$F_0/F = 1 + K_Q[Q] \quad (2)$$

Alternatively, a modified Stern–Volmer equation was used [35]:

$$F_0/\Delta F = 1/([Q] f_a K_{Q(eff)}) + 1/f_a \quad (3)$$

in which case [Q] is the concentration of quencher, $K_{Q(eff)}$ is the effective quenching constant, f_a is the effective fractional maximum accessible fluorescence, F_0 is the fluorescence in the absence of quencher, and ΔF is the difference in fluorescence in the presence and absence of quencher [35]. The data were fitted to the above equations by simple linear regression.

Urea-denaturation studies

FABP (1 μM final concn.) was diluted into 50 mM Hepes buffer, pH 7.5 (25 °C), and the sample allowed to equilibrate (as monitored by fluorescence emission). Urea (9.6 M stock solution in buffer) was added in aliquots (50–100 μl). After equilibration tryptophan fluorescence (excitation at 280 nm, emission at 330 nm) was averaged over a 60 s interval. Data were corrected for dilution effects.

Effect of fatty acid binding on quenching of tryptophan fluorescence

FABP (1 μM final concn.) was diluted into 50 mM Hepes buffer, pH 7.5 (25 °C), and the sample allowed to equilibrate (as monitored by fluorescence emission). Fatty acids and fatty acid metabolites (0.1 or 1.0 mM stock solution in methanol) were added in aliquots (0.2–2 μl). After equilibration tryptophan fluorescence (excitation at 280 nm, emission at 330 nm) was averaged over a 60 s interval. Data were corrected for dilution effects.

Energy transfer

Non-radiative energy transfer is defined as the transfer of excited state energy from a donor to an acceptor and is dependent, among other factors, on the distance between these molecules [33,36]. Försters theory [37] defines the efficiency of energy transfer (E) as follows:

$$E = R^{-6}/(R^{-6} + R_0^{-6}) \quad (4)$$

where R_0, the distance at which energy transfer efficiency is 50% (Förster distance), is given by:

$$R_0 = (JK^2 Q Y_0 n^{-6})^{1/6} \times 9.7 \times 10^3 \text{ Å} \ (1 \text{ Å} = 0.1 \text{ nm}) \quad (5)$$

in which case K^2 is the orientation factor for dipole–dipole interactions, QY_0 is the quantum yield in the absence of energy acceptor and n is the refractive index of the medium between the donor and acceptor [36].

For energy transfer to take place the fluorescence emission spectrum of the donor must overlap the absorption spectrum of the acceptor, as measured by the spectral overlap integral J [36,38]:

$$J = [\int F(\lambda)\epsilon(\lambda)\lambda^4 \Delta\lambda]/[\int F(\lambda)\Delta\lambda] \quad (6)$$

where $F(\lambda)$ is the fluorescence intensity of the energy donor at wavelength λ, $\epsilon(\lambda)$ is the absorption coefficient ($M^{-1}\cdot cm^{-1}$) of

the energy acceptor, and $\Delta\lambda$ is the interval of measurement (5 nm).

The efficiency of energy transfer (E) was calculated from the quantum yield of the energy donor (protein) in the presence (QY_T) and absence (QY_0) of the energy acceptor, DAUDA [36]:

$$E = 1 - QY_T/QY_0 \quad (7)$$

where QY_T and QY_0 are the quantum yields in the presence and absence of the energy acceptor (DAUDA).

The relevant quantum yields were determined as follows:

$$QY_{sample} = QY_{std} \times F_{sample}/F_{std} \times I_{std}/I_{sample} \times A_{std}/A_{sample} \quad (8)$$

where QY is the relevant quantum yield of the standard or sample, F is the relative fluorescence determined by integrating the area under the corrected fluorescence spectrum, I is the relative light intensity at the excitation wavelength and A is the absorbance at the excitation wavelength [38,39]. In both cases the same excitation wavelength (280 nm) was used and therefore $I_{std}/I_{sample} = 1$. The fluorescence emission was measured between 300 and 350 nm. Tryptophan in water ($QY = 0.19$) was used as the quantum yield standard [38].

For aligned and parallel dipoles the variation in K^2 results in only 26% error in R [33]. In many cases the donor and acceptor molecules undergo fast Brownian motion during the lifetime of the donor [40]. Therefore the donor and acceptor rotate freely in a time that is short compared with the excited state lifetime of the donor and K^2 is equal to two-thirds [36]. For the purpose of energy-transfer calculations it was therefore assumed that K^2 is 0.667 [36,38] and the refractive index is 1.4 [41].

The fraction of FABP forming a complex with DAUDA was calculated from the following equation [47]:

$$2[EL]/[E_0] = (1 + [L_0]/[E_0] + K_D/[E_0]) - \{(1 + [L_0]/[E_0] + K_D/[E_0])^2 - 4[L_0]/[E_0]\}^{\frac{1}{2}} \quad (9)$$

Where $[E_0]$ is the concentration of protein in the absence of ligand and [EL] is the concentration of protein containing bound ligand. Under the assumption that $[E_0] = 0.05\ \mu M$, $[L_0] = 5\ \mu M$ and $K_D = 0.50\ \mu M$, the proteins were determined to be fully saturated with the energy acceptor, DAUDA, and therefore no corrections for fractional saturation ($f_{sat} = [EL]/[E_0]$, $E_{corr} = E_{obs}/f_{sat}$) were required [41].

Protein modelling

Protein structures were imported from the Brookhaven database and used on the molecular graphics software QUANTA (Polygen Corp., Waltham, MA, U.S.A.) on a Silicon Graphics computer system. Inter-atomic distances were determined using the relevant algorithms provided by the software. The intestinal FABP structure has been published [1,9].

RESULTS

Binding of fluorescent fatty acid analogues

The fluorescent fatty acid analogue, DAUDA, bound to FABP with a resultant blue-shift of the fluorescence emission maxima and increase in fluorescence quantum yield (Table 1), as shown previously [42]. The emission maxima for the C69W and F18W proteins were lower and higher respectively as compared with the wild-type protein. Dissociation constants (K_D) were decreased for the F3W and C69W proteins, while the maximum calculated fluorescence ($B_{max.}$) was decreased for the F3W protein and increased for the C69W mutant, as compared with the wild-type protein (Table 1). The dissociation constants obtained for DAUDA are similar to values we have obtained previously [11] and equivalent to the values of 0.24 μM, 0.72 μM and 0.64 μM obtained with DAUDA, 16-anthroyloxypalmitate and 1-pyrenedodecanoic acid respectively [10]. Similar observations were made with DPH-PA as fluorophore (Table 2). In this case the relative changes in $B_{max.}$ observed with DAUDA for F3W and C69W were confirmed with DPH-PA, although the K_D values were equivalent for all the proteins.

Table 1 Fluorescence properties of DAUDA binding to FABP

DAUDA fluorescence (excitation at 350 nm, emission at 500 nm) was determined in the absence or presence of FABP (0.05 μM). DAUDA concentrations were varied (0–5 μM) and the data fitted to a hyperbolic equation using non-linear regression [50] to determine the values of B_{max} (arbitrary units) and K_D (μM) ± S.E.M. Results shown of one experiment which is representative of multiple experiments. The values of emission wavelength maxima [$\lambda_{max.}$(emission)] were determined by adding aliquots of FABP to a 0.3 μM solution of DAUDA. The number of data points for emission-maxima measurements are shown in parentheses.

	$B_{max.}$	K_D	$\lambda_{max.}$(emission) (nm)
DAUDA	–	–	543 ± 1.2 (6)
FABP			
WT	46 ± 2	0.58 ± 0.09	496 ± 1.1 (6)*
F3W	28 ± 2	0.30 ± 0.08	498 ± 2.2 (6)*
F18W	48 ± 1	0.46 ± 0.05	500 ± 1.5 (6)†
C69W	55 ± 2	0.36 ± 0.05	491 ± 1.1 (6)*†

*$P < 0.001$, relative to buffer control.
†$P < 0.001$, relative to wild-type FABP.

Table 2 Fluorescence properties of DPH-PA binding to FABP

DPH-PA fluorescence (excitation at 360 nm, emission at 430 nm) was determined in the absence and presence of FABP (0.05 μM). DPH-PA concentrations were varied (0–5 μM) and the data fitted to a hyperbolic equation using non-linear regression [50] to determine the values of $B_{max.}$ (arbitrary units) and K_D (μM) ± S.E.M. Results are from one experiment which is representative of multiple experiments.

FABP	$B_{max.}$	K_D (μM)
WT	111 ± 15	1.20 ± 0.33
F3W	77 ± 16	1.11 ± 0.42
F18W	109 ± 15	1.16 ± 0.22
C69W	142 ± 9	1.31 ± 0.14

An attempt to determine *cis*-parinaric acid binding parameters under steady-state conditions resulted in significant fluorescence bleaching and/or ligand dissociation with time. Therefore no further attempts were made to determine K_D or $B_{max.}$ values using this probe. Under identical experimental conditions *cis*-parinaric acid did bind to human serum albumin in a manner that resulted in an increased and constant fluorescence emission (results not shown). Though binding of *cis*-parinaric acid to wild-type FABP has been reported previously, these measurements were made under fast-reaction kinetic conditions [8].

DAUDA displacement by oleate

Under conditions of apparently equimolar concentrations of FABP and DAUDA the relative displacement of DAUDA by oleate was similar for all the proteins (Figure 1). However, under these conditions the fluorescence of DAUDA bound to the F3W and C69W proteins was significantly lower and higher respectively than for the comparable wild-type or F18W proteins

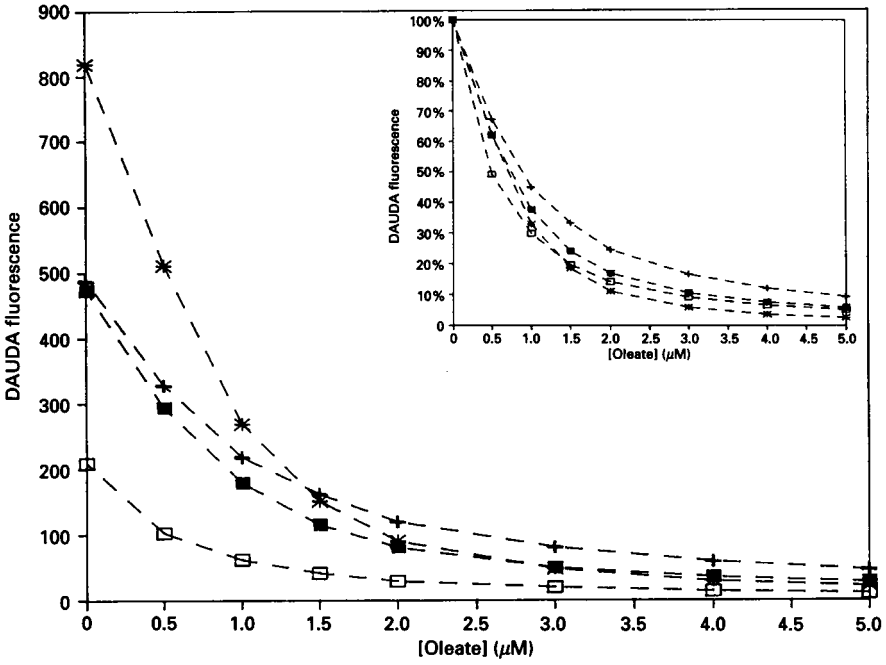

Figure 1 Displacement of DAUDA by oleate

Samples contained 1 μM protein and 1 μM DAUDA, with oleate (in methanol) added in aliquots. Fluorescence was measured at an excitation wavelength of 350 nm and an emission wavelength of 500 nm. The inset shows fluorescence emission data as a percentage of the initial fluorescence. ■, WT; □, F3W; +, F18W; *, C69W.

(Figure 1). These results would appear to confirm the above binding parameters obtained with DAUDA and DPH-PA (Tables 1 and 2).

Fluorescence quenching by acrylamide

Fluorescence quenching by acrylamide indicated that the tryptophans in the different proteins were partially solvent-accessible. The quenching constants for the F3W, F18W and C69W proteins, calculated from a modified Stern–Volmer equation [35], were 38 ± 8, 48 ± 2 and $34 \pm 3\ M^{-1}$, and the effective fractional accessible fluorescence values were 0.62 ± 0.13, 0.55 ± 0.04 and 0.75 ± 0.07 respectively. Thus the C69W tryptophan appeared to be the most solvent-accessible with the lowest quenching constant, whereas the F18W tryptophan displayed the lowest effective fractional accessibility value and the highest quenching constant. It should be noted that Cys-69 of the wild-type protein is partially accessible to DTNB [17], in agreement with the acrylamide quenching results. Although the charged environment surrounding the relative tryptophans can be investigated using I^- and Cs^+ ions, these studies were complicated by an ionic strength effect as displayed by apparent quenching in the presence of comparative KCl concentrations (results not shown).

Urea-denaturation studies

Protein-denaturation studies in the presence of urea show differential effects of the three tryptophan mutants to protein unfolding (Figure 2). Tryptophan fluorescence, unlike tyrosine fluorescence, is affected by solvent polarity and can therefore be used as a measure of protein denaturation [33]. The F18W mutant showed the lowest, and the C69W protein the highest, apparent midpoint of transition expressed as concentration of urea (C_m). Both the F18W and C69W proteins appeared to demonstrate simple sigmoidal unfolding kinetics whereas the F3W protein possibly displays a biphasic denaturation curve under equilibrium conditions. No attempt has been made to calculate thermodynamic or kinetic parameters from these data due to the inherent complexity of kinetic models for protein denaturation [43,44] and the relative lack of data points (Figure 2). Although Gibbs-free-energy (ΔG_D) changes for protein unfolding can be calculated by linear extrapolation of denaturation profiles [45], the assumption of linearity is only valid for proteins undergoing folding transitions in the 0–2 M urea concentration range [44].

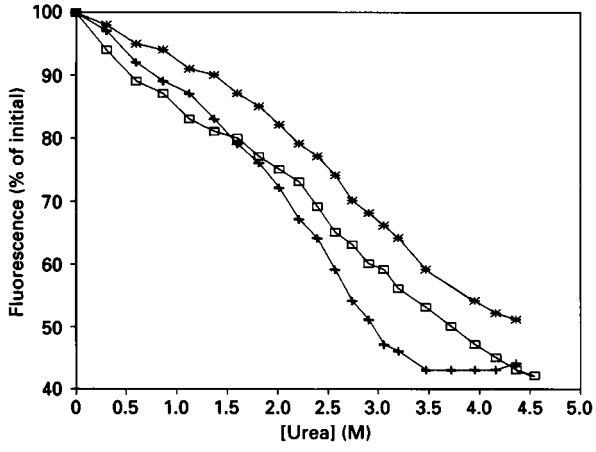

Figure 2 Urea denaturation of FABP mutants (1 μM protein)

Urea was added in aliquots and fluorescence measured at an excitation wavelength of 280 nm and an emission wavelength of 330 nm. □, F3W; +, F18W; *, C69W.

Table 3 Effect of different substrates on tryptophan fluorescence

Samples contained 1 μM FABP and 2 μM ligand (in 2 μl of methanol) was added. Tryptophan fluorescence (excitation at 280 nm, emission at 330 nm) was measured and the above values are percentages of the fluorescence in the presence of a 2-fold excess of ligand relative to the initial fluorescence. Values shown are those of separate experiments or means ± S.D. (n).

	Percentage of initial fluorescence (%)		
Substrate	F3W	F18W	C69W
Methanol	98, 97	98, 95	98, 97
Oleate	102, 101	107, 106	89, 92
Stearate	97.0 ± 1.0 (3)	103.3 ± 1.5 (3)	90, 97
Palmitate	94, 95	113, 109	94, 91
Oleoyl-lysoPC	92, 96	104, 105	92, 95
Oleoyl-CoA	89, 86	88.7 ± 2.5 (3)	78, 82
9(10)-Bromostearate	97, 100	108.7 ± 0.6 (3)	92, 93
2-Bromopalmitate	79.0 ± 2.6 (3)	70.0 ± 6.6 (4)	84.5 ± 2.0 (4)

Table 4 Tryptophan fluorescence quenching by 2-bromopalmitate

Samples contained 1 μM FABP, and 2-bromopalmitate (in methanol) was added in aliquots. Tryptophan fluorescence (excitation at 280 nm, emission at 330 nm) was measured after sample equilibration. The quenching constants (K_Q) ± S.E.M. were determined by linear regression using the Stern–Volmer (K_Q) [34] or modified Stern–Volmer ($K_{Q(eff)}$) equations [35]. The effective fractional maximum fluorescence (f_a) for the modified Stern–Volmer equation is shown in parentheses [35]. Data were not corrected for the effect of palmitate. Results for two experiments are shown.

	Quenching constant (μM^{-1})		
Equation	F3W	F18W	C69W
Stern–Volmer	0.24 ± 0.005	0.15 ± 0.002	0.25 ± 0.05
Modified Stern–Volmer	0.65 ± 0.03 (0.44 ± 0.01)	0.20 ± 0.03 (0.85 ± 0.19)	0.83 ± 0.11 (0.32 ± 0.04)

Effect of fatty acids on tryptophan fluorescence:

In general, the addition of ligands to the F3W or C69W mutants showed no apparent effects on tryptophan fluorescence although an increase was observed with the F18W protein (Table 3). In contrast, there was a notable decrease in fluorescence for all three mutants upon addition of oleoyl-CoA.

The two brominated fatty acids, 2-bromopalmitate and 9(10)-bromostearate, had apparently contrasting effects (Table 3). Bromostearate showed no effect on fluorescence when compared with stearate, but fluorescence quenching was observed with bromopalmitate, the greatest effect obtained with the F18W protein (Figure 3; Tables 3 and 4). The effective fractional saturation value for the F18W protein was not significantly different from unity, whereas it was less than 50% for the other two mutants. However, the F3W protein was quenched slightly better than the C69W protein (Table 4), which was also reflected by comparison of the relative difference in the effect of palmitate and 2-bromopalmitate on tryptophan fluorescence, i.e. an approximate decrease of 15% and 8% respectively (Table 3).

Energy transfer

All three tryptophan mutants (F3W, F18W, C69W) showed typical tryptophan emission spectra when excited at 280 nm with

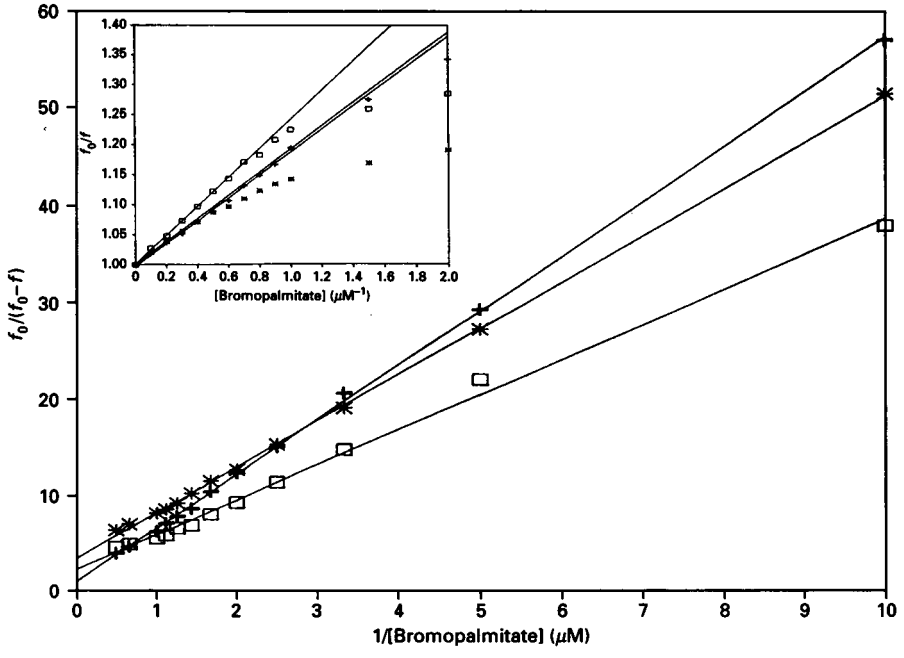

Figure 3 Quenching of tryptophan fluorescence by 2-bromopalmitate

Samples contained 1 μM protein and the 2-bromopalmitate was added in aliquots. Fluorescence was measured at an excitation wavelength of 280 nm and an emission wavelength of 330 nm. The data were fitted to a modified Stern–Volmer equation. The inset shows the same data fitted to the Stern–Volmer equation with the lines indicating the initial linear regions of the curves. □, F3W; +, F18W; *, C69W.

Table 5 Fluorescence energy transfer determinations with the fluorophore DAUDA

Quantum yields (*QY*), efficiency of energy transfer (*E*), overlap integral (*J*), Förster distance (R_0) and the distances between the centres of donor and acceptor chromophores ($R_{obs.}$) were determined as described. Results shown are from one experiment. In these studies the concentration of FABP was 0.05 μM (energy donor) and of DAUDA 5 μM (energy acceptor). (Note: 1 Å = 0.1 nm.)

FABP	*QY*	E_{obs}	$10^{15} \times J$	R_0 (Å)	R_{obs} (Å)
WT	0.009	–	–	–	–
F3W	0.018	0.93	6.0	3.6	10.3
F18W	0.081	0.95	5.8	3.6	12.3
C69W	0.025	0.94	5.8	3.6	10.7

emission maxima between 320 and 340 nm (results not shown), thus displaying a blue-shift in emission relative to tryptophan in water, where the fluorescence maximum is 348 nm [46].

The wild-type FABP contains three tyrosines but no tryptophans [3], and this is reflected by the low quantum yield of this protein relative to the three tryptophan mutants (Table 5). The F18W mutant has a significantly higher quantum yield than the other two tryptophan mutants, but all three tryptophan mutants displayed similar energy-transfer efficiencies and *R* values, the distance between donor and acceptor chromophores (Table 5). No energy transfer was detected for the wild-type protein.

Previously published quantum yields for intestinal FABP tryptophan and liver FABP tyrosine were 0.294 and 0.0658 respectively [8]. As shown, the quantum yield for wild-type FABP was 0.009 (Table 5), which reflects a 7-fold difference in quantum yield values for rat liver FABP obtained in this paper and the above published values. As R_0 depends on the sixth root of the quantum yield, it is not very sensitive to uncertainties in the donor quantum yield [40]. The average value for *R*, approx. 1 nm (10 Å) (Table 5), calculated for the three tryptophan mutants probably reflects the relatively small size of the FABP protein (15 kDa) and a position of the fluorescent moiety of DAUDA in the binding cavity.

Analysis of the intestinal FABP crystal structure using a molecular-graphics system revealed that the three amino acids mutated in this study are approximately equidistant from each other, the respective C_α carbons separated by the following distances: C_α-2–C_α-17 = 2.42 nm (24.2 Å), C_α-2–C_α-68 = 1.95 nm (19.5 Å), C_α-17–C_α-68 = 2.28 nm (22.8 Å). Sequence analysis has shown that Phe-3 and Phe-18 are analogous in intestinal and liver FABP, while Phe-69 of intestinal FABP is replaced by a cysteine in rat liver FABP [3] and therefore, based on the assumption that the two structures are equivalent, it can be postulated that these amino acids are probably also equidistant in liver FABP (no structure has been published for liver FABP). On the basis of this hypothesis and the results of the energy-transfer studies it can therefore be concluded that the naphthyl moiety of the DAUDA probe is buried in the β-clam cavity of the protein.

DISCUSSION

In this study three rat liver FABP amino acids, i.e. Phe-3, Phe-18 and Cys-69, were replaced with tryptophans to facilitate studies of ligand binding and protein structure.

Binding of three fluorescent fatty acid analogues to the FABP mutant proteins has been investigated. The proteins showed emission maxima for DAUDA binding between 490 nm and 500 nm (Table 1). All the proteins displayed similar binding affinities, although there was a significant decrease in the $B_{max.}$ value for the F3W protein. Analysis of binding by the fluorescent fatty acid analogues DAUDA and DPH-PA (Tables 1 and 2) have been interpreted to show essentially the same binding affinity for both probes, although there is a consistent decrease in $B_{max.}$ for F3W, while this parameter is slightly increased in the case of C69W. A number of factors can affect the fluorescence emission intensity of a fluorophore, including the polarity of the environment, mobility of the fluorophore and a change in intermolecular quenching by the protein, and hence changes in $B_{max.}$ are difficult to interpret. However, the C69W protein displayed an increased $B_{max.}$ value (relative to wild-type protein), which possibly reflects an increase in binding-site hydrophobicity as reflected by the increased blue-shift observed with C69W and DAUDA (Table 1). A simple explanation for the increased hydrophobicity with the C69W mutation is that a cysteine has been replaced by a tryptophan.

The displacement of DAUDA from FABP by oleate, which is a competitive inhibitor of DAUDA binding [11], shows that the relative effect is equivalent for the four proteins (Figure 1). However, the changes in $B_{max.}$ values, discussed above, are reflected in a plot of actual fluorescence values (Figure 1), thus confirming the results obtained with DAUDA and DPH-PA.

Urea-denaturation studies indicate a subtle change in susceptibility to denaturation for the mutant proteins (Figure 2). The following model has been proposed for intestinal FABP unfolding under equilibrium conditions [43]:

$$\text{Native} \rightarrow \text{intermediate} \rightarrow \text{unfolded} \quad (10)$$

It was proposed by Ropson et al. [43] that the two protein domains surrounding Trp-6 and Trp-82 in intestinal FABP, i.e. the β-A and β-F chains, respectively [1,9], could unfold independently. In the case of the rat liver FABP it is tempting to speculate that there is a two-intermediate step in protein unfolding. As shown by the fluorescence change in the F3W protein (Figure 2) the β-A chain could be destabilised to a small degree before the rest of the β-clam structure and α-helical portal domains unfold, the latter unfolding step also being detected in the F18W (portal region) and C69W (β-clam) regions. Therefore the following reaction scheme can be proposed:

$$\text{Native} \rightarrow \text{intermediate 1 } (\beta\text{-A chain}) \rightarrow \text{intermediate 2 (portal and } \beta\text{-clam)} \rightarrow \text{unfolded} \quad (11)$$

Though kinetic studies by Ropson et al. [43] were interpreted to indicate multiple refolding pathways in rat intestinal FABP, similar conclusions in this study would require a more detailed analysis.

The binding of various ligands to FABP resulted in diverse effects on tryptophan fluorescence (Table 3). In general, no effect was observed for the F3W or C69W proteins, while there was a consistent increase in fluorescence for the F18W mutant with the exception of oleoyl-CoA binding. In intestinal FABP Phe-18 is located in the α-helical domain, and structural changes of this domain have been observed between the apo- and holo-structures [1,9,48]. Thus the increased fluorescence observed with F18W could possibly be explained by such changes in protein structure. The decrease in fluorescence obtained with oleoyl-CoA for all three mutants can be explained by the increased size of this molecule, in relation to fatty acids, therefore causing a greater distortion in protein configuration.

Investigations with 9(10)-bromostearate and 2-bromopalmitate revealed greater quenching with the latter compound for the F18W protein over and above the quenching seen at the other

positions (Figure 3; Tables 3 and 4). Therefore it can be argued that Trp-18 is close to the carboxy moiety of at least one bound fatty acid. By contrast, the bromine located in the middle of the stearate acyl chain displayed no quenching effect when compared with stearate (Table 3), thus having no direct contact with any of the mutated tryptophans.

Energy-transfer studies showed that the fluorescent moiety of DAUDA is approximately equidistant from the three tryptophans (Table 5). Investigation of the intestinal FABP structure using a molecular-graphics system indicate that the C_α atoms of the relevant amino acids in intestinal FABP, i.e. Phe-3, Phe-18 and Phe-69, are also virtually equidistant. Thus it can be inferred that the fluorescent moiety of DAUDA, which is bound in a 1:1 stoichiometry to liver FABP [42], is located within the β-clam.

Analysis of the energy transfer studies and the crystal structure of intestinal FABP leads to the conclusion that the fluorescent moiety of the DAUDA probe is probably located in the β-clam, or solvent cavity, of the protein. Fluorescence quenching studies with bromopalmitate indicate that at least one fatty acid carboxylate is located near the portal region with the acyl chain within the β-clam structure. This interpretation would explain the solvent-accessibility of fatty acid carboxylates bound to liver FABP [6,7] and the ability of liver FABP to bind ligands with bulky headgroups [49]. However, in this situation the fatty acids would be accommodated in a different orientation from that shown for intestinal FABP [9].

In conclusion, it has been shown that the tryptophan mutants of rat liver FABP, i.e. F3W, F18W and C69W, generally display the same binding properties, although there are subtle differences in susceptibility to urea denaturation. Energy-transfer and fluorescence-quenching studies appear to show that ligands bind to liver FABP in a different configuration to intestinal FABP, thus apparently substantiating previous findings showing differences in binding properties between intestinal and liver FABP. Further studies are in progress to investigate more closely the exact nature of ligand interactions with rat liver FABP.

Financial support from the Wellcome Trust is gratefully acknowledged.

REFERENCES

1 Sacchettini, J. C., Gordon, J. I. and Banaszak, L. J. (1989) J. Mol. Biol. **208**, 327–339
2 Kaikaus, R. M., Bass, N. M. and Ockner, R. K. (1990) Experientia **26**, 617–630
3 Veerkamp, J. H., Peeters, R. A. and Maatman, R. G. H. J. (1991) Biochim. Biophys. Acta **1081**, 1–24
4 Sweetser, D. A., Heuckeroth, R. O. and Gordon, J. I. (1987) Annu. Rev. Nutr. **7**, 337–359
5 Lowe, J. B., Sacchettini, J. C., Laposata, M., McQuillan, J. J. and Gordon, J. I. (1987) J. Biol. Chem. **262**, 5931–5937
6 Cistola, D. P., Sacchettini, J. C., Banaszak, L. J., Walsh, M. T. and Gordon, J. I. (1989) J. Biol. Chem. **264**, 2700–2710
7 Cistola, D. P., Walsh, M. T., Corey, R. P., Hamilton, J. and Brecher, P. (1988) Biochemistry **27**, 711–717
8 Nemecz, G., Jefferson, J. R. and Schroeder, F. (1991) J. Biol. Chem. **266**, 17112–17123
9 Sacchettini, J. C., Scapin, G., Gopaul, D. and Gordon, J. I. (1992) J. Biol. Chem. **267**, 23534–23545
10 Peeters, R. A., In'T Groen, A. M. P., De Moel, M. P., Van Moerkerk, H. T. B. and Veerkamp, J. H. (1989) Int. J. Biochem. **21**, 407–418
11 Thumser, A. E. A., Evans, C., Worrall, A. F. and Wilton, D. C. (1993) Biochem. J. **297**, 103–107
12 Burrier, R. E. and Brecher, P. (1986) Biochim. Biophys. Acta **879**, 229–239
13 Jakoby, M. J., Miller, K. R., Toner, J. J., Bauman, A., Cheng, L., Li, E. and Cistola, D. P. (1993) Biochemistry **32**, 872–878
14 Peeters, R. A., Veerkamp, J. H., van Kessel, A. G., Kanda, T. and Ono, T. (1991) Biochem. J. **276**, 203–207
15 Scapin, G., Spadon, P., Mammi, M., Zanotti, G. and Monaco, H. (1990) Mol. Cell. Biochem. **98**, 95–99
16 Zanotti, G., Scapin, G., Spadon, P., Veerkamp, J. H. and Sacchettini, J. C. (1992) J. Biol. Chem. **267**, 18541–18550
17 Wilton, D. C. (1989) Biochem. J. **261**, 273–276
18 Evans, C. and Wilton, D. C. (1990) Mol. Cell. Biochem. **98**, 135–140
19 Maniatis, T., Fritsch, E. F. and Sambrook, J. (1982) Molecular Cloning: A Laboratory Manual, Cold Spring Harbor Laboratory Press, Cold Spring Harbor, NY
20 Messing, J. (1983) Methods Enzymol. **101**, 20–78
21 Kunkel, T. A., Roberts, J. D. and Zakour, R. A. (1987) Methods Enzymol. **154**, 367–382
22 Sanger, F., Nicklen, S. and Coulson, A. R. (1977) Proc. Natl. Acad. Sci. U.S.A. **74**, 5463–5467
23 Brown, T. A. (1991) Essential Molecular Biology: A Practical Approach, vol. 1 (Brown, T. A., ed.), p. 253, IRL Press, Oxford
24 Worrall, A. F., Evans, C. and Wilton, D. C. (1991) Biochem J. **278**, 365–368
25 Glatz, J. F. C. and Veerkamp, J. H. (1983) Anal. Biochem. **132**, 89–95
26 Bradford, M. (1976) Anal. Biochem. **72**, 248–254
27 Laemmli, U. K. (1970) Nature (London) **227**, 680–685
28 Haugland, R. P. (1992) Handbook of Fluorescent Probes and Research Chemicals, 5th edn. (Larison, K. D., ed.), Molecular Probes, Eugene, OR
29 Trotter, P. J. and Storch, J. (1989) Biochim. Biophys. Acta **982**, 131–139
30 Sklar, L. A., Hudson, B. S., Petersen, M. and Daimond, J.(1977) Biochemistry **16**, 813–818
31 Prendergast, F. G., Haugland, R. P. and Callahan, P. J.(1981) Biochemistry **20**, 7333–7338
32 Roberts, G. C. K. (1983) in Standards in Fluorescence Spectroscopy (Miller, J. N., ed.), pp. 49–64, Chapman and Hall, London
33 Lakowicz, J. R. (1983) Principles of Fluorescence Spectroscopy, Plenum Press, New York
34 Stern, O. and Volmer, M. (1919) Phys. Z. **20**, 183
35 Lehrer, S. S. (1971) Biochemistry **10**, 3254–3263
36 Stryer, L. (1978) Annu. Rev. Biochem. **47**, 819–846
37 Förster, T. (1948) Ann. Physik **2**, 55–75
38 Lee, A. G. (1982) Lipid. Membr. Biochem. **B422**, 1–49
39 Pesce, A. J., Rosen, C. G. and Pasby, T. L. (1971) Fluorescence Spectroscopy: An Introduction for Biology and Medicine (Pesce, A. J., ed.), Marcel Dekker Inc., New York
40 Steinberg, I. Z. (1971) Annu. Rev. Biochem. 40, 83–114
41 Fairclough, R. H. and Cantor, C. R. (1978) Methods Enzymol. **48**, 347–379
42 Wilkinson, T. C. I. and Wilton, D. C. (1986) Biochem. J. **238**, 419–424
43 Ropson, I. J., Gordon, J. I. and Frieden, C. (1990) Biochemistry **29**, 9591–9599
44 Staniforth, R. A., Burston, S. G., Smith, C. J., Jackson, G. S., Badcoe, I. G., Atkinson, T., Holbrook, J. J. and Clark, A. R. (1993) Biochemistry **32**, 3842–3851
45 Bolen, D. W. and Santoro, M. M. (1988) Biochemistry **27**, 8069–8074
46 Teale, F. J. W. and Weber, G. (1957) Biochem. J. **65**, 476–482
47 Snyder, B. and Hammes, G. G. (1984) Biochemistry **23**, 5787–5795
48 Scapin, G., Gordon, J. I. and Sacchettini, J. C. (1992) J. Biol. Chem. **267**, 4253–4269
49 Sheridan, M. and Wilton, D. C. (1992) FEBS Lett. **314**, 486–488
50 Leatherbarrow, R. (1987) Enzfitter software, Elsevier Biosoft, Cambridge
51 Motulsky, H. J. and Ransnas, L. A. (1987) FASEB J. **1**, 365–374

Received 11 October 1993/26 January 1994; accepted 3 February 1994